ICCPGE 2016, 1, 25 - 30

Performance Analysis of Shell and Tube Heat Exchanger Using Different Correlations at Mellitah Complex

Abosalah ElMehdi*
Department of Mechanical Engineering, University of Zawia, Sabratha, Libya
*Corresponding Author: hakeem_sasy@yahoo.com

Abstract

Shell-and-tube heat exchangers are used extensively in the chemical process industries, especially in refineries and other large chemical process, because of the numerous advantages they offer compare to the other types. In this paper, a comparative analysis of rich amine and lean amine shell and tube heat exchanger were made. All measurements are collected from a heat exchanger using three of 1-2 shell and tube heat exchanger in series installed at the process facility of Sulfur recovery unit situated at the Mellitah complex. Rich amine is the cold fluid which flows inside the tubes. However; lean amine serves as hot fluid inside the shell is made. The aim of this study to see what is the difference between the design condition and the operation condition. The evaluation of convective heat transfer coefficients and pressure drops for different mass flow rates and inlet and outlet temperatures are presented using various correlations, so the various performance parameters such as overall heat transfer coefficient, effectiveness and pressure drop obtained through experiments is compared with the values obtained from both the different correlations and the design basis. An Excel program was developed for the ease of calculation and obtaining results of both shell and tube side fluids.

Keywords: Shell and tube heat exchanger; performance analysis; overall heat transfer coefficient; effectiveness.

Nomenclature	
$T_{h,i}$	Shell-side inlet temperature (^{O}C)
$T_{h,o}$	Shell-side outlet temperature (^{O}C)
$T_{c,i}$	Tube side inlet temperature (^{O}C)
$T_{c,o}$	Tube side outlet temperature (^{O}C)
$\triangle T_{lm}$	Log mean temperature difference (^{O}C)
$U_{o,c}$	Theoretical overall heat transfer coefficient (W/m²K)
$U_{o,m}$	eExperimental overall heat transfer coefficient (W/m²K)
h_o	Outside heat transfer coefficient (W/m²K)
h_i	Inside heat transfer coefficient (W/m²K)
K	Thermal conductivity of heat exchanger wall (W/mK)
R_{e_i}	Reynolds number of tube side
R_{e_o}	Reynolds number of shell side

1. Introduction

A heat exchanger is a device that is used to transfer energy or exchange the heat between two fluids one is hot and the other is cold, each fluid does not mix with the other. There are many applications that use a heat exchanger: heating the feed water on a boiler, the oil cooler on an aircraft engine, and the air conditioning system. There are two ways in which heat is transferred in the heat exchanger: conduction through the wall that separates the two fluids and convection in each fluid [1]. There are three basic types of heat exchangers: Recuperators:- In this type of heat exchanger the hot and cold fluids are separated by a wall and heat is transferred by a combination of convection to and from the wall and conduction through the wall. The wall can include extended surfaces, such as fins or other heat transfer enhancement devices.

Regenerators: - In a regenerator the hot and cold fluids alternately occupy the same space in the exchanger core. The exchanger core or "matrix" serves as a heat storage device that is periodically heated by the warmer of the two fluids and then transfers heat to the colder fluid. In a fixed matrix configuration, the hot and cold fluids pass alternately through a stationary exchanger, and for continuous operation two or more matrices are necessary. One commonly used arrangement for the matrix is the "packed bed". Another approach is the rotary regenerator in which a circular matrix rotates and alternately exposes a portion of its surface to the hot and then to the cold fluid [8].

Direct Contact Heat Exchangers: - In this type of heat exchanger the hot and cold fluids contact each other directly. An example of such a device is a cooling tower in which a spray of water falling from the top of the tower is directly contacted and cooled by a stream of air flowing upward. Other direct contact systems use immiscible liquids or solid-to-gas exchange [8].

A more common type of heat exchanger that is widely used in the chemical and process industry is the shell-and-tube arrangement. In this type of heat exchanger one fluid flows inside the tubes while the other fluid is forced through the shell and over the outside of the tubes. The fluid is forced to flow over the tubes rather than along the tubes because a higher heat transfer coefficient can be achieved in cross-flow than in flow parallel to the tubes. To achieve cross-flow on the shell side, baffles are placed inside the shell. These baffles ensure that the flow passes across the tubes in each section, flowing downward in the first, upward in the second, and so on. Depending on the header arrangements at the two ends of the heat exchanger, one or more tube passes can be achieved. For a two-tube-pass arrangement, the inlet header is split so that the fluid flowing into the tubes passes through half of the tubes in one direction, then turns around and returns through the other half of the tubes to where it started. Three- and four-tube passes can be achieved by rearrangement of the header space [4]. The main objective of the study is to evaluate the performance parameters of a counter flow shell and tube heat exchanger like overall heat transfer coefficient, effectiveness and pressure drop obtained through experiments is compared with the values obtained from both the different correlations and the design basis.

2. Material and Methods

For all these types, there are two methods of analysis: The log mean temperature difference (LMTD) method, and the number of transfer units (NTU) which is based on a formal definition of effectiveness [2]. The LMTD method can be readily used when the inlet and outlet temperatures of both the hot and cold fluids are known. When the outlet temperatures are not known, the LMTD can only be used in an iterative scheme. In this case the effectiveness-NTU method can be used to simplify the analysis.

2.1. Performance analysis of shell and tube heat exchanger

2.1.1. Actual rate of heat transfer ($\dot{Q}$)

The actual heat transfer rate (heat duty) can be defined from an energy balance of the cold fluid or the hot fluid which means the heat transfer rate of the hot fluid is equal to the heat transfer rate of the cold fluid according to the first law of thermodynamics.

$$\dot{Q} = C_h(T_{h,i} - T_{h,o}) = C_c(T_{c,o} - T_{c,i}) \qquad (2.1)$$

Where heat capacity rate for hot or cold fluid is

$$\dot{C} = mC_p \qquad (2.2)$$

But experimentally the heat may loss or gain to or from the surrounding.

2.1.2. Overall heat transfer coefficient

The thermal performance of the shell and tube heat exchanger will be calculated in this paper. A convenient parameter to examine for this matter is the overall heat transfer coefficient, U. In the following different variations of U will be explained. These parameters are plotted in a diagram showing the thermal performance of the heat exchanger. The first explained parameter is the measured heat transfer coefficient Umeasured.

- Measured heat transfer coefficient

Measured heat transfer coefficient is predicted by using the duty of the heat exchanger. The duty is calculated by using Equation 2.1. The overall heat transfer coefficient is calculated by the equation.

$$U_{o,m} = \frac{\dot{Q}}{AF\triangle T_{lm}} \qquad (2.3)$$

Where F is versus two temperature ratios P and R defined as

$$P = \frac{T_{c,o} - T_{c,i}}{T_{h,i} - T_{c,i}} \tag{2.4}$$

$$R = \frac{T_{h,i} - T_{h,o}}{T_{c,o} - T_{c,i}} \tag{2.5}$$

The mathematical relationships between R, P and F can be found in Kern books Figure (20), the log mean temperature difference ($\triangle T_{lm}$) for counter flow is :

$$\triangle T_{lm} = \frac{(T_{h,i} - T_{c,i}) - (T_{h,o} - T_{c,i})}{ln\left[(T_{h,i} - T_{c,o})/(T_{h,o} - T_{c,i})\right]} \tag{2.6}$$

- Design heat transfer coefficient

The design U is here defined as the overall heat transfer coefficient required to cool the fluid as specified in the design basis. It can be calculated from design condition of heat duty and the log mean temperature difference as following:

$$U_{o,d} = \frac{\dot{Q}_{design}}{AF\triangle T_{lm,_{design}}} \tag{2.7}$$

- Corrected heat transfer coefficient

A corrected heat transfer coefficient for clean surfaces can be defined as conduction resistance of a solid wall and convection resistance of hot fluid and cold fluid using different correlations of Nusselt number, and needs to be modified to account for the effects of fouling on both the inner and the outer surfaces of the tube. The following correlation for U is expressed based on the out surface area.

$$U_{o,c} = \frac{A_o}{h_i A_i} + \frac{A_o R_{f,i}}{A_i} + \frac{ln\left(\frac{d_o}{d_i}\right)}{2\pi KL} + R_{f,o} + h_o \tag{2.8}$$

Nusselt number for the inside flow can be calculated using the following correlations for in-tube heat transfer

(a) Dittus-Boelter, 1930 $for\ R_{e_i} > 10^4$:[6]

$$Nu_i = 0.023 R_{e_i}^{0.8} P_{r_i}^{0.4}\ for\ R_{e_i} > 10^4 \tag{2.9}$$

(b) Gnielinski, 1976 $for\ 3\times10^3 < R_{e_i} < 5\times10^6$:[7]

$$Nu_i = \frac{(f/8)R_{e_i} - 1000)P_{r_i}}{1 + 12.7(f/8)^{0.5}(P_{r_i}^{\frac{2}{3}} - 1)} \tag{2.10}$$

(c) Petukhov, 1970 $for 10^4 < R_{e_i} < 5\times10^6$:

$$Nu_i = \frac{(f/8)R_{e_i} P_{r_i}}{1.07 + 12.7(f/8)^{0.5}(P_{r_i}^{\frac{2}{3}} - 1)} \tag{2.11}$$

Where:

$$f = (0.79\, ln\, R_e - 1.64)^{-2}\, for\ 10^4 < R_e < 10^6 \tag{2.12}$$

The Nusselt number correlation for average heat-transfer coefficients in flow across tube banks is

$$Nu_o = C R_{e_{o,max}}^n P_{r_o}^{\frac{1}{3}} \tag{2.13}$$

Where the constants C and n are tabulated in Table 6-4 (Holman).

$$R_{e_{o,max}}^n = \frac{\rho_o \nu_{o,max} d_o}{\mu_o} \tag{2.14}$$

$$\nu_{o,max} = \frac{u_\infty S_n}{S_n - d_o} \tag{2.15}$$

2.1.3. Effectiveness of the heat-exchanger (ε)

The effectiveness of the heat-exchanger is defined as the ratio of the actual heat transfer rate to the maximum possible heat transfer rate.

$$\varepsilon = \frac{\dot{Q}}{\dot{Q}_{max}} \tag{2.16}$$

Where:

$$\dot{Q}_{max} = C_{min}\left(T_{h,i} - T_{c,i}\right) \tag{2.17}$$

$$C_{min} = min\left(C_h, C_c\right) \tag{2.18}$$

2.1.4. Pressure Drop

- Tube-Side Pressure Drop

Calculation of the tube-side pressure drop is made by first estimating the (Darcy) friction factor for flow through the tubes from the value of the Reynolds number and the relative roughness, and applying the viscosity correction can be calculated from Equation 2.12.

$$\triangle P = 4f\,\frac{L}{d_i}\frac{\rho_i \nu_i^2}{2} \times Np \tag{2.19}$$

Kern correlation

$$\triangle P = \left[4f\,\frac{LNp}{d_i} + 4Np\right]\frac{\rho_i \nu_i^2}{2} \tag{2.20}$$

- Shell-Side Pressure Drop

Calculation of the shell-side pressure drop is made by Kays and London correlation.

$$\triangle P = f \, \frac{A_o}{A_{min}} \, \frac{\rho_o \nu_o^2}{2} \tag{2.21}$$

2.1.5. Detailed description of equipment and experimental procedure

The experimental takes place at sulfur recovery unit situated at the Mellitah complex. The rich amine leaving the bottom of the MDEA Absorber is sent to the MDEA Regenerator through the lean/rich heat exchangers where, the rich MDEA, is heated from 50 °C to 100 °C by cooling the lean MDEA which is leaving the regenerator from 129 °C to 78 °C. All measurements are collected from a heat exchanger using three of 1-2 Shell and Tube Heat Exchanger in series during the months of (August and November).

3. Results and Discussion

Figures 2.1 and 3.2 show the variation of overall heat transfer coffeicient with mass flow rate of cold fluid (tube side) for August and November, 2015 respectively. It can be seen that the theoretical overall heat transfer coefficient increases with increasing mass flow rate. It is due to the fact that with increasing mass flow rate the Reynolds number increases and as a result Nusselt number also increases which is directly proportional to heat transfer coefficient, so the overall heat transfer coffeicient increases.

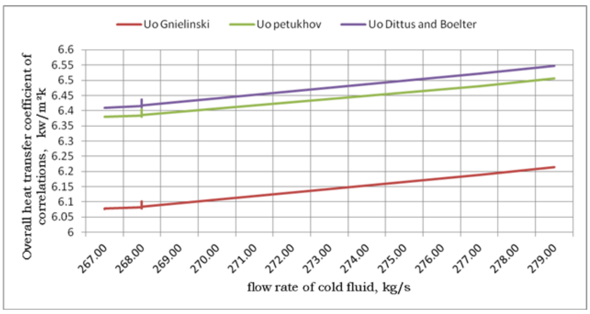

Figure 3.1: Variation of overall heat transfer coefficient of different correlations with mass flow rate of cold fluid for August, 2015

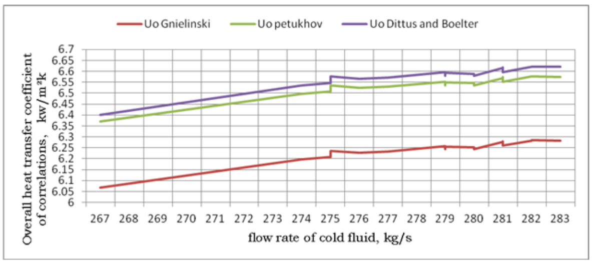

Figure 3.2: Variation of overall heat transfer coefficient of different correlations with mass flow rate of cold fluid for Novmber, 2015

Figures 3.3 and 3.4 above show the development of the effetiveness with time for August and November, 2015 respectively. Both measured ε and corrected ε are plotted. It is observed that the design ε is lower than both measured ε and corrected ε in the actual time period, because the design conditions of outlet temperature are different compare to the measured one.

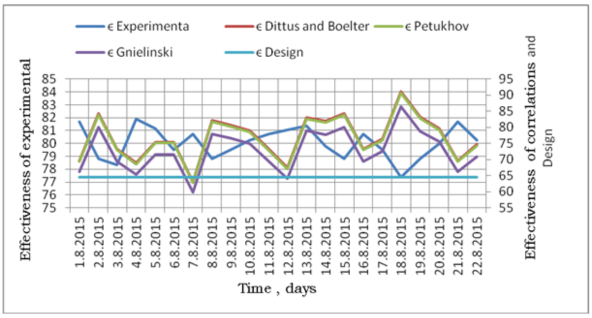

Figure 3.3: Variation of effectiveness with time for August, 2015

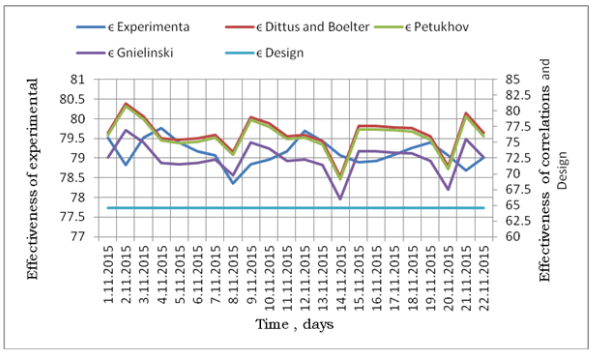

Figure 3.4: Variation of effectiveness with time for November, 2015

It is clear from the diagram that the corrected ε for

Table 3.1: Design conditions

Quantity	T_i,°C	T_o,°C	$\dot{m}$, kg/s	$\triangle p$, bar	$\dot{Q}$, KW	U_d , KW/m^{2}K	ε_d,%
Rich amine	48	100	348.23	7.1	67854	3.11	64.53
Lean amine	129	78	337.19	1.25	67854	3.76	64.53

Table 3.2: Evaluation of the Performance Analysis for expermintal data and different correlation for August 2015

Date	$T_{i,h}$,	$T_{o,h}$,	$T_{i,c}$,	$T_{o,c}$,	$\dot{m}$,	$\dot{m}$,	$\triangle T_{lm}$	$U_{o,m}$	$U_{o,D}$	$U_{o,P}$	$U_{o,G}$
Day	^oC	^oC	^oC	^oC	$\frac{kg}{s}$	$\frac{kg}{s}$		$\frac{KW}{m^2K}$	$\frac{KW}{m^2K}$	$\frac{KW}{m^2K}$	$\frac{KW}{m^2K}$
1	127	63	45	112	258.61	268.33	16.45	7.51	6.41	6.38	6.08
2	129	64	44	111	259.16	268.05	18.98	5.99	6.41	6.38	6.08
3	128	62	45	110	258.88	268.05	17.49	6.85	6.41	6.38	6.07
4	127	62	44	112	258.88	268.05	16.45	7.62	6.41	6.38	6.07
5	128	63	44	112	258.88	268.05	17.92	6.90	6.41	6.38	6.07
6	128	63	45	111	259.16	268.05	17.49	6.76	6.41	6.38	6.08
7	128	60	45	112	259.16	268.05	15.49	8.20	6.41	6.38	6.08
8	129	63	44	111	259.16	268.05	18.49	6.15	6.41	6.38	6.08
9	128	64	45	111	259.16	268.05	17.98	6.31	6.41	6.38	6.08
10	129	64	44.3	112	261.94	268.05	18.92	6.53	6.43	6.40	6.10
11	127	63	44	111	259.16	268.05	17.45	7.07	6.41	6.38	6.08
12	129	63	44.6	113	262.22	277.5	17.17	7.82	6.52	6.48	6.18
13	128.8	66	43	112.8	263.33	279.44	19.28	6.40	6.54	6.50	6.21
14	128	64	44	111	259.16	268.05	18.45	6.24	6.41	6.38	6.08
15	128	63	43	110	258.88	267.77	18.98	5.98	6.41	6.37	6.07
16	127	62	44	111	259.16	267.5	16.98	7.05	6.41	6.37	6.07
17	128	63	45	111	259.16	268.05	17.49	6.67	6.41	6.38	6.08
18	129	65	45	110	259.44	268.05	19.49	5.44	6.41	6.38	6.08
19	129	64	44	111	258.61	268.05	18.98	6.07	6.41	6.37	6.07
20	128	64	43	111	258.61	268.05	18.92	6.43	6.41	6.37	6.07
21	127	63	45	112	258.61	268.33	16.45	7.51	6.41	6.38	6.08
22	129	62	43	112	259.16	268.33	17.98	6.88	6.41	6.38	6.08

Table 3.3: The other evaluation of the Performance Analysis parameters for August 2015

Date Day	ε_m, %	ε_D, %	ε_P, %	ε_G, %	$\triangle P_{t,\,darcy}$, bar	$\triangle P_{t,\,kern}$, bar	$\triangle P_{S,kays\ and\ london}$, bar
1	81.70	69.71	69.37	66.10	3.24	3.39	0.427
2	78.82	84.35	83.94	79.79	3.24	3.39	0.429
3	78.31	73.30	72.95	69.50	3.24	3.39	0.428
4	81.92	68.94	68.61	65.36	3.24	3.39	0.428
5	81.17	75.43	75.07	71.52	3.24	3.39	0.428
6	79.51	75.42	75.06	71.51	3.24	3.39	0.429
7	80.72	63.09	62.78	59.81	3.24	3.39	0.429
8	78.82	82.19	81.79	77.92	3.24	3.39	0.429
9	79.51	80.75	80.36	76.56	3.24	3.39	0.429
10	80.23	79.04	78.65	74.92	3.24	3.39	0.437
11	80.72	73.17	72.81	69.37	3.24	3.39	0.429
12	81.04	67.52	67.10	64.07	3.44	3.60	0.438
13	81.35	83.14	82.59	78.89	3.48	3.64	0.441
14	79.76	81.91	81.51	77.66	3.24	3.39	0.429
15	78.82	84.38	83.97	79.99	3.23	3.38	0.428
16	80.72	73.30	72.95	69.49	3.23	3.38	0.429
17	79.51	76.47	76.10	72.50	3.24	3.39	0.429
18	77.38	91.16	90.71	86.42	3.24	3.39	0.430
19	78.82	83.18	82.77	78.86	3.24	3.39	0.427
20	80	79.63	79.24	75.50	3.24	3.39	0.427
21	81.70	69.71	69.37	66.10	3.24	3.39	0.427
22	80.23	74.77	74.40	74.40	3.24	3.39	0.429

the three correlations increase and decrease with the same range and the reason is the difference of the operation condition during this time.
Figures 3.5 and 3.6 show how the pressure drop in the heat exchanger varies with varying mass flow rate and also the comparison between design and theoretical pressure drop. It can be seen that the pressure drop increases with mass flow rate for each case. However the design pressure drop is much more as compared to the theoretical pressure drop because the mass flow rate in design condition is more than in operation condition, so the theoretical calculations of the pressure drop decrease as well as velocity decrese. Also the pressure drops at the entrance and the header have not been calculated.

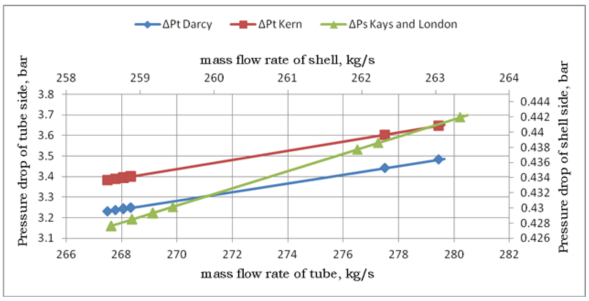

Figure 3.5: Variation of pressure drop with mass flow rate for August, 2015

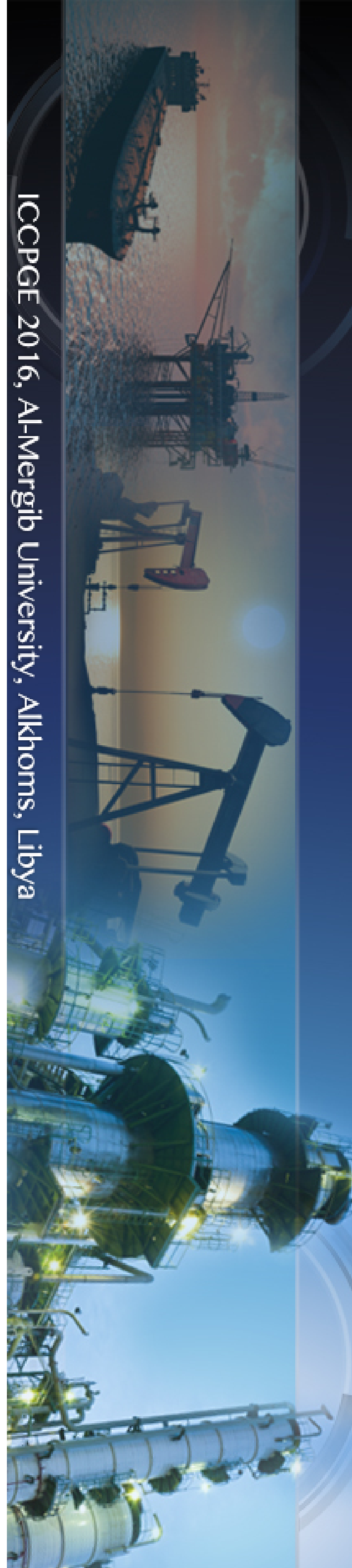

Table 3.4: Evaluation of the Performance Analysis for expermintal data and different correlation for Novmber 2015

Day	$T_{i,h}$ ^oC	$T_{o,h}$, ^oC	$T_{i,c}$, ^oC	$T_{o,c}$ ^oC	$\dot{m}$, $\frac{kg}{s}$	$\dot{m}$, $\frac{kg}{s}$	$\triangle T_{lm}$	$U_{o,m}$ $\frac{KW}{m^2K}$	$U_{o,D}$ $\frac{KW}{m^2K}$	$U_{o,P}$ $\frac{KW}{m^2K}$	$U_{o,G}$ $\frac{KW}{m^2K}$
1	127	62	44	110	258.33	267.22	17.49	6.64	6.40	6.37	6.06
2	128	62	43	110	258.33	267.22	18.49	6.21	6.40	6.37	6.06
3	127	62.7	44	110	258.33	267.22	17.83	6.43	6.40	6.37	6.06
4	128	62	44	111	258.33	267.22	17.49	6.75	6.40	6.37	6.06
5	128	63.6	45.5	111	268.33	267.22	17.54	6.97	6.61	6.57	6.28
6	127.8	63.5	45.7	110.7	269.44	283.05	17.44	6.93	6.62	6.57	6.28
7	128	61.8	43.4	110.3	268.61	282.22	18.04	6.83	6.59	6.55	6.25
8	128.1	62.5	44.5	110	268.88	279.72	18.04	7.05	6.62	6.57	6.28
9	128.3	62.1	43.7	110.4	268.05	282.77	18.14	6.55	6.57	6.53	6.23
10	128.2	64.1	46.4	111	269.16	277.77	17.44	6.69	6.61	6.50	6.27
11	128	63.4	45.4	110.8	269.72	281.66	17.59	6.89	6.61	6.57	6.27
12	127.8	62.8	44.6	110.9	270.55	281.11	17.54	6.87	6.57	6.53	6.23
13	127.7	61.4	43.1	110.3	270	275.83	17.84	6.98	6.51	6.57	6.28
14	128.7	63.6	46.5	111.5	269.16	281.38	17.14	7.49	6.59	6.55	6.25
15	128.3	61.5	43.5	110.4	269.77	279.44	17.94	6.69	6.58	6.54	6.25
16	129	61.5	43.1	110.9	267.5	280	18.24	6.71	6.60	6.55	6.26
17	127.8	60.6	41.7	109.8	267.22	274.16	18.44	6.67	6.53	6.49	6.19
18	127.9	62.3	43.5	110.4	268.05	276.94	18.14	6.73	6.56	6.52	6.22
19	127.7	63.4	45.2	110.7	266.66	280	17.59	6.87	6.58	6.53	6.24
20	127.9	61.9	43.8	110.3	267.22	275.55	17.84	7.26	6.54	6.50	6.20
21	128.2	62.8	44.2	110.3	267.22	279.44	18.24	6.49	6.57	6.53	6.24
22	127.3	60.5	41.5	109.3	266.94	281.66	18.49	6.81	6.59	6.55	6.26

Table 3.5: The other evaluation of the Performance Analysis parameters for Novmber 2015

Day	ε_m, %	ε_D, %	ε_P, %	ε_G, %	$\triangle P_{t,\,darcy}$, bar	$\triangle P_{t,\,kern}$, bar	$\triangle P_{S,kays\ and\ london}$, bar
1	79.51	76.54	76.18	72.56	3.22	3.37	0.426
2	78.82	81.18	80.79	76.96	3.22	3.37	0.426
3	79.51	79.10	87.73	74.99	3.22	3.37	0.426
4	79.76	75.63	75.27	71.70	3.22	3.37	0.426
5	79.39	75.40	74.87	71.55	3.56	3.72	0.457
6	79.17	75.59	75.07	71.73	3.54	3.71	0.460
7	79.07	76.23	75.73	72.32	3.48	3.65	0.458
8	78.34	73.50	72.99	69.75	3.55	3.72	0.459
9	78.84	79.06	78.56	74.99	3.44	3.60	0.456
10	78.97	78.02	77.49	74.03	3.53	3.63	0.459
11	79.17	76.00	75.48	72.10	3.51	3.68	0.461
12	79.86	76.20	75.74	72.25	3.40	3.56	0.464
13	79.43	75.23	74.72	71.37	3.52	3.69	0.462
14	79.07	69.54	69.09	65.97	3.48	3.64	0.459
15	78.89	77.58	77.07	73.61	3.49	3.66	0.455
16	78.92	77.55	77.02	73.59	3.53	3.69	0.454
17	79.09	77.41	76.96	73.40	3.37	3.52	0.453
18	79.26	77.25	76.77	73.27	3.42	3.59	0.456
19	79.39	75.97	75.47	72.08	3.49	3.66	0.452
20	79.07	71.20	70.77	67.52	3.39	3.55	0.453
21	78.69	79.69	79.15	75.59	3.48	3.64	0.453
22	79.02	76.53	76.01	72.63	3.53	3.69	0.453

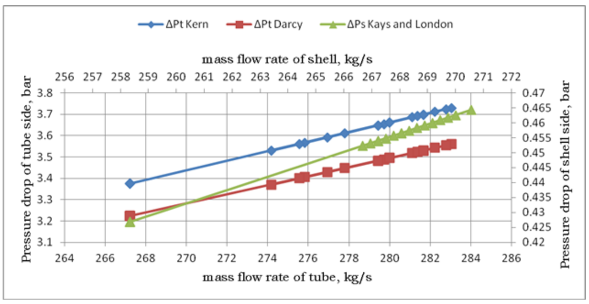

Figure 3.6: Variation of pressure drop with mass flow rate for November, 2015

4. conclusion

The study is conducted to determine the thermal performance parameters of the shell and tube of heat exchanger at different operation condition. It is found in both months that the overall heat transfer coefficient by different correlations that obtained by using the simulation software (Excel) increase with increasing mass flow rate. The results were almost the same if we compare between the experimental results and the theoretical results, so the range of the overall heat transfer coefficient of experimental for both months was between (5.4 - 7.9KW/m^{2}K), however for the theoretical correlations was between (6.06 - 6.6KW/m^{2}K). Also the pressure drop increases with increasing mass flow rate and the design values are more as compared to theoretical results because the mass flow rate in design condition is about 1.5 more than in operation condition which effect on the velocity. Also the design overall heat transfer coefficient is less than the experimental, it is about half of the experimental value because the ΔTlm of the design condition is about twice of the experimental, the reason is the outlet temperatures for both cold and hot fluid of the design condition were not the same as the experimental condition.

Acknowledgment

The authors acknowledge the support given for this work by the operation department of Sulfur recovery unit at the Mellitah complex. Also the support of the staff faculty of the Subratha engineering faculty.

References

[1] Yunus A Cengel.: "Heat Transfer a Practical Approach," 2nd .ed. McGraw-Hill Book Company, New York, 1998.

[2] B.K. HODGE.: "Analysis and Design of Energy System," 3rd. ed., Prentice-Hall, Inc. A Viacom Company, New Jersey, 1999

[3] W. M. Kays and A. L. London.: "Compact Heat Exchangers," 3rd .ed. McGraw-Hill Book Company, New York, 1984

[4] P. Holman, Heat Transfer, 9th Edition, McGraw-Hill, 2002

[5] D. Q. Kern, Process Heat Transfer, McGraw-Hill, New York, 1950

[6] Dittus, F.W. and L.M.K. Boelter. 1930. Heat transfer in automobile radiators of the tubular types, University of California Publication Engineering, 12:443

[7] Gnielinski, V. 1976. New equation for heat and mass transfer in turbulent pipe and channelow, Int. Chem. Eng., 16(2) : 359-368

[8] Frank Kreith; Raj M. Manglik; and Mark S. Bohn.: "Principles of Heat Transfer," 7th ed. Cengage Learning, Inc, 2011